Single-particle and collective excitations in the transitional nucleus ^{166}Os

S Stolze[1]‡ T Grahn[1]§, R Julin[1], D T Joss[2], K Andgren[3], K Auranen[1], S Bönig[4], D Cox[1], I G Darby[2], M Doncel[3], S Eeckhaudt[1], P T Greenlees[1], B. Hadinia[3], A Herzáň[1,5], U Jakobsson[1], P Jones[1], S Juutinen[1], S Ketelhut[1], J Konki[1], T Kröll[4], A-P Leppänen[1], M Nyman[1], R D Page[2], J Pakarinen[1], J Partanen[1], C G McPeake[2], D O'Donnell[2], P Peura[1], P Rahkila[1], P Ruotsalainen[1], M Sandzelius[1], J Sarén[1], B Saygı[2], C Scholey[1], J Simpson[6], J Sorri[1], M J Taylor[7], A Thornthwaite[2] and J Uusitalo[1]

[1] University of Jyvaskyla, Department of Physics, P. O. Box 35, FI-40014 University of Jyvaskyla, Finland

[2] Department of Physics, Oliver Lodge Laboratory, University of Liverpool, Liverpool, L69 7ZE, United Kingdom

[3] Department of Physics, Royal Institute of Technology, SE-10691, Stockholm, Sweden

[4] Institut für Kernphysik, TU Darmstadt, 64289 Darmstadt, Germany

[5] Institute of Physics, Slovak Academy of Sciences, SK-84511 Bratislava, Slovakia

[6] STFC Daresbury Laboratory, Daresbury, Warrington, WA4 4AD, United Kingdom

[7] Department of Physics and Astronomy, University of Manchester, Manchester M13 9PL, United Kingdom

Abstract.

The mean lifetimes of the lowest energy 2^+, 8^+ and 9^- states in ^{166}Os have been measured using the recoil distance Doppler-shift method in conjunction with a selective recoil-decay tagging technique. These measurements extend studies into the most neutron-deficient mass region accessible to current experimental methods. The $B(E2; 2^+ \rightarrow 0^+) = 7(2)$ W.u. extracted from these measurements is markedly lower than those observed in the heavier even-mass Os isotopes. The 8^+ and 9^- states yield reduced transition probabilities that are consistent with single-particle transitions. While these values may indicate a departure from collective structure, the level scheme and the underlying nuclear configurations can also be interpreted in terms of a simple collective picture. This contrasting behaviour suggests an intriguing dichotomy in the description of heavy transitional nuclei.

Keywords: Mean lifetimes, RDDS measurements, gamma-ray spectroscopy, collectivity,

‡ Present address: Physics Division, Argonne National Laboratory, 9700 South Cass Ave, Argonne, IL 60439, United States

§ Corresponding author, email: tuomas.grahn@jyu.fi

single-particle states, electromagnetic transitions

1. Introduction

The systematic variation of nuclear properties across a complete shell can reveal the development of collective behaviour arising from correlated nucleon motion. The evolution of collectivity is reflected in the changes of low-lying excited states as a function of nucleon number. For example, the excitation energy of the first 2^+ state is correlated with the proximity of an even-even nucleus to a closed shell. The excitations of the nucleus are characterised by 2^+ states with large excitation energies arising from single-particle excitations near the shell closure, which fall gradually with the addition of valence nucleons to a minimum at the mid shell. Nuclei are usually well deformed at the mid shell and consequently excited states form rotational bands that are built on top of their band-head configurations.

In osmium nuclei, excited states have been identified in the isotopes spanning the range from $^{162}Os_{86}$ [1] to $^{198}Os_{122}$ [2], which covers almost all known osmium isotopes and most of the $82 \leq N \leq 126$ shell. Rotational excitations based on axially deformed shapes dominate the yrast line at low spin in the Os nuclei around the neutron mid shell at $N = 104$. The identification of excited states in the more neutron-deficient transitional isotopes approaching the $N = 82$ closed shell has been made possible by the exploitation of the selective recoil-decay tagging technique [3]. While the evolution of excitation energies provide useful insights into the onset of collectivity, more detailed information about the nuclear matrix elements can be obtained by measuring lifetimes of excited states.

Recent lifetime measurements of the low-lying yrast states in the neutron-deficient W, Os and Pt isotopes have revealed some anomalous features. Ratios of reduced transition probabilities derived from mean lifetime measurements in the $N = 94$ isotones ^{172}Pt [4] and ^{170}Os [5], and the $N = 92$ isotones ^{168}Os [6] and ^{166}W [7] are found to be significantly lower than the values predicted by collective models.

Recent measurements of odd-A nuclei suggest that the anomaly in the even-even core may arise due to the soft triaxial shapes of these nuclei [8] but there are also scenarios that can explain such anomalous ratios with $B(E2; 4^+ \rightarrow 2^+)/B(E2; 2^+ \rightarrow 0^+) < 1$ in terms of $I = 0$ seniority coupling [9, 10]. The intriguing dichotomy is that such interpretations are typically reserved for nuclei near closed shells and are not usually invoked for nuclei like the heavy $N = 92$ isotones, which have sufficient valence nucleons to generate collective excitations. Low ratios of reduced transition probabilities have been observed in other mass regions and a consistent explanation of this phenomenon has not been determined.

It is desirable to obtain further information on the properties of the transitional Os isotopes to help to understand this phenomenon. This paper reports the results of two recoil-decay tagging experiments to probe the structure of the neutron-deficient nucleus $^{166}Os_{90}$. The mean lifetimes τ have been extracted for the yrast 2^+, 8^+ and 9^- states

and the level scheme has been extended to high spin ($I = 18$).

2. Experimental details

The structure of ^{166}Os was studied in two experiments carried out at the Accelerator Laboratory of the University of Jyväskylä, Finland. The first experiment synthesised ^{166}Os in an excited state via the ^{92}Mo(^{78}Kr,$2p2n$) reaction at beam energies of 357 MeV and 368 MeV. The ^{92}Mo target had a nominal thickness of 0.5 mg cm^{-2} in both experiments. Gamma rays were detected at the target position with the Jurogam I γ-ray spectrometer comprising a total of 43 Eurogam Phase 1 [11] type and GASP [12] Compton-suppressed germanium detectors. The recoiling fusion-evaporation residues were separated from the primary beam with the RITU gas-filled separator [13, 14] and implanted into the double-sided silicon strip detectors (DSSD) of the GREAT spectrometer [15] located at the RITU focal plane. The fusion-evaporation residues were discriminated from scattered beam and target-like nuclei by their time of flight between the multi-wire proportional counter (MWPC) and the DSSD and their energy-loss characteristics in the MWPC. All of the detector channels were read out independently and time-stamped relative to a 100 MHz clock signal in the Total Data Readout data acquisition system [16]. The events were reconstructed offline in the Grain [17] software package using spatial and temporal correlations. The $\gamma\gamma$ coincidence matrices were analyzed with the Radware software package [18, 19].

The ^{92}Mo(^{78}Kr,$2p2n$) reaction at a bombarding energy of 380 MeV was used to synthesise ^{166}Os nuclei in the second experiment. This experiment used the Jurogam II γ-ray spectrometer, which comprised 15 Eurogam Phase 1 type Compton-suppressed Ge detectors [11] in two rings (with $\theta = 133^\circ$ and 157° with respect to the beam axis) and 24 Eurogam Compton-suppressed clover detectors [20] positioned in two rings around 90°. The segmentation of the clover detectors was used to form four rings with angles $\theta = 71^\circ,\ 80^\circ,\ 100^\circ$ and 109°. The DPUNS differential plunger [21] was installed at the target position. The stretched ^{92}Mo target was used with a 1 mg cm^{-2} Mg degrader foil slowing the velocity of the recoiling ions from $v/c = 4.2\%$ to 3.3%. The relative distance between the target and degrader foils could be adjusted and measured precisely by a capacitance measurement. A total of nine target-to-degrader distances ranging from 8 µm to 8000 µm were utilised to cover the region of sensitivity for the lowest excited states.

3. Results

3.1. Level scheme

Gamma-ray transitions in ^{166}Os were identified using the recoil-decay tagging technique [3]. This method matches γ rays emitted at the target position to specific nuclei implanted in the focal-plane DSSD and their subsequent radioactive decays using spatial and temporal correlations. The ground-state α decay of ^{166}Os ($E_\alpha = 6548$ keV)

with its short half-life (181 ms) and high α-decay branching ratio [22] is ideal for recoil-decay tagging.

A total of 1.6×10^6 ^{166}Os α-decay correlated $\gamma\gamma$-coincidences were detected in the first experiment. The time for recoil-α(^{166}Os) correlations within the same DSSD pixel was limited to 600 ms corresponding to approximately three half-lives. This total includes recoil-decay correlations with escaping ^{166}Os α particles that deposit only a fraction of their energy in the detector. Escaping ^{166}Os α particles were selected by decay correlations with the full-energy α decay of its decay product ^{162}W, in the same DSSD pixel within 2 s. Typical α-decay correlated γ-ray coincidence spectra are shown in figure 1. The level scheme was extended and ordered on the basis of γ-ray coincidences, energy sums and relative intensities.

The properties of γ rays assigned to ^{166}Os are listed in table 1 and the extended level scheme is shown in figure 2. Due to the presence of self-coincident γ-ray doublets and insufficient counting statistics it has not been possible to determine the multipolarities for all but the most intense transitions. Consequently, the spin assignments for most levels are tentative.

Table 1: The energies and intensities (relative to the 2^+ state) of the γ rays observed at the Jurogam I target position. Due to the long lifetime of the 9^- state at 2801 keV, the sum of the observed intensities of the transitions feeding this state is higher than that of the de-exciting 442 keV transition.

E_γ (keV)	I_γ (%)	E_i (keV)	$I_\mathrm{i} \rightarrow I_\mathrm{f}$
169.6 (8)	9.1(1)	2971	$(10^-) \rightarrow (9^-)$
204.5(6)	2.1(2)	1929	$(5^-) \rightarrow (6^+)$
313.9(6)	3(3)	4585	$(15) \rightarrow (14)$
320.4(6)	1.5(2)	4905	$(16) \rightarrow (15)$
368.1(6)	18.2(8)	1929	$(5^-) \rightarrow (3^-)$
389.3(7)	1.2(2)	5295	$(17) \rightarrow (16)$
430.0(6)	16.5(8)	2359	$(7^-) \rightarrow (5^-)$
432.0(6)	100(5)	432	$2^+ \rightarrow 0^+$
442.4(6)	12.8(5)	2801	$(9^-) \rightarrow (7^-)$
476.5(6)	2.8(3)	3707	$(12) \rightarrow (10)$
481.9(8)	18.6(11)	3453	$(12^-) \rightarrow (10^-)$
495.3(8)	12.5(3)	3397	$(11^-) \rightarrow (9^-)$
509.1(12)	6.5(10)	3310	$(11^-) \rightarrow (9^-)$
510.4(6)	14.6(7)	2861	$(10^+) \rightarrow (8^+)$
520.3(12)	0.5(3)	3400	$(11^-) \rightarrow (9^-)$
520.7(12)	10.2(6)	2880	$(9^-) \rightarrow (7^-)$
540.6(6)	13.4(8)	1561	$(3^-) \rightarrow 4^+$
543.6(12)	1.2(4)	3854	$(13^-) \rightarrow (11^-)$

E_γ (keV)	I_γ (%)	E_i (keV)	$I_\mathrm{i} \rightarrow I_\mathrm{f}$
563.3(7)	0.8(2)	4271	$(14) \rightarrow (12)$
575.4(9)	0.5(3)	5284	$(18^-) \rightarrow (16^-)$
583.9(8)	7.9(6)	4037	$(14^-) \rightarrow (12^-)$
588.4(6)	86(4)	1020	$4^+ \rightarrow 2^+$
597.9(8)	7.1(5)	3895	$(13^-) \rightarrow (11^-)$
610.4(8)	4(4)	4505	$(15^-) \rightarrow (13^-)$
615.8(8)	6.2(5)	4069	$(14^-) \rightarrow (12^-)$
625.2(8)	1.3(3)	5130	$(17^-) \rightarrow (15^-)$
626.1(6)	24.2(10)	2350	$(8^+) \rightarrow (6^+)$
657.4(6)	9(4)	3518	$(12^+) \rightarrow (10^+)$
672.1(8)	1.3(3)	4709	$(16^-) \rightarrow (14^-)$
697.5(8)	3.4(4)	4766	$(16^-) \rightarrow (14^-)$
703.8(6)	41(2)	1724	$6^+ \rightarrow 4^+$
722.7(10)	0.8(3)	5489	$(18^-) \rightarrow (16^-)$
739.3(7)	1.8(3)	4257	$(14^+) \rightarrow (12^+)$
752.9(6)	1.8(2)	4271	$(14) \rightarrow (12^+)$
780.3(6)	3.4(4)	2505	$(8^+) \rightarrow 6^+$
811.1(7)	2(3)	3316	$(10^+) \rightarrow (8^+)$
880.5(7)	0.8(3)	3231	$(10) \rightarrow (8^+)$
909.3(6)	4.7(4)	1929	$(5^-) \rightarrow 4^+$
1128.5(6)	4.5(4)	1561	$(3^-) \rightarrow 2^+$

The ground-state band in ^{166}Os (band 1) was first observed by King *et al.* [23]. In the present work, the ground-state band has been extended to the non-yrast $I^\pi = (10^+)$ state and is displayed through coincidences with the 811 keV transition in figure 1(c). Appelbe *et al.* [24] extended the yrast cascade to spin $I = 14$ and an excited band was assigned firmly to ^{166}Os. The assignment of γ rays to ^{166}Os reported in reference [24] is confirmed in the present work although the ordering of the 510 keV and 657 keV γ-ray transitions has been exchanged and the tentative second excited band in reference [24] is not observed in the present work. Gamma rays in coincidence with the 626 keV transition highlighting the yrast band (band 2) are shown in figure 1(b). Figure 1(d) shows γ rays in coincidence with the 314 keV transition indicating another band that has parallel decay paths to the yrast (12^+) and (8^+) states of band 2. Figure 1(f) shows the γ-ray spectrum obtained by demanding coincidences with the 442 keV γ-ray transition, which shows the side band (band 4) identified in reference [24]. Several new high-spin structures, notably bands 5, 6 and 7, are observed to feed into band 4. The γ-ray spectra generated from coincidences with transitions from these cascades are shown in figure 1(g) and figure 1(h).

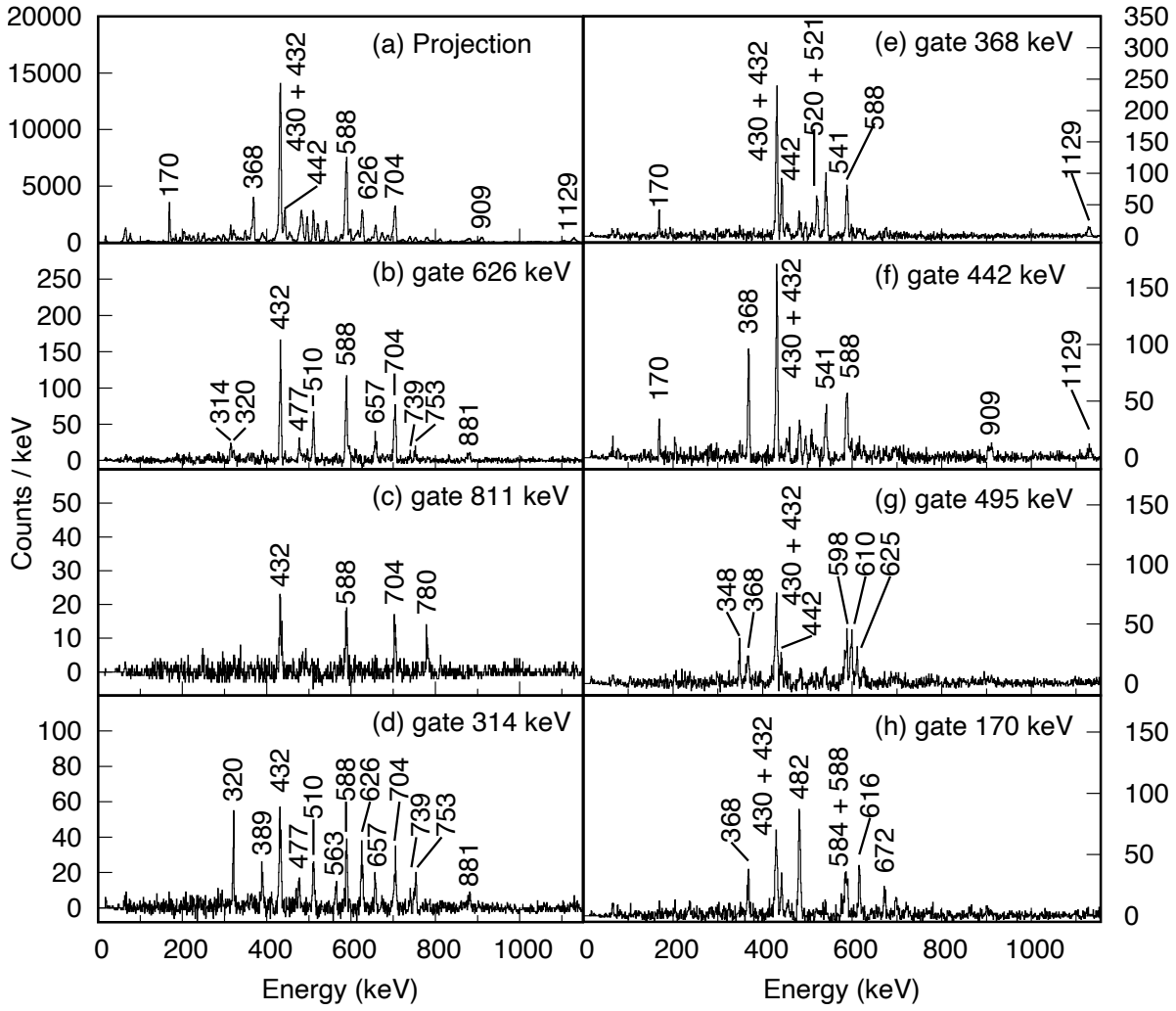

Figure 1. (a) The total projection of the ^{166}Os α-decay correlated $\gamma\gamma$ matrix. A search time of 600 ms was used to correlate the α particles and recoils detected in the same DSSD pixel. In (b)-(h) same conditions are required. The most intense peaks are labelled. (b) The γ rays in coincidence with the 626 keV γ ray. (c) The γ rays in coincidence with the 811 keV γ ray. (d) The dipole band structure, in coincidence with the 314 keV γ ray. (e) The γ rays in coincidence with the 368 keV γ ray showing the feeding from the negative-parity band to the ground-state band. (f) The γ rays in coincidence with the 442 keV γ ray depopulating the long-lived (9^-) state. (g) The continuation of the negative-parity band in coincidence with the 495 keV γ ray. The origin of the 348 keV γ-ray could not be confirmed and thus it is not placed in the level scheme. (h) The γ rays in bands 6 and 7 in coincidence with the connecting 170 keV γ ray.

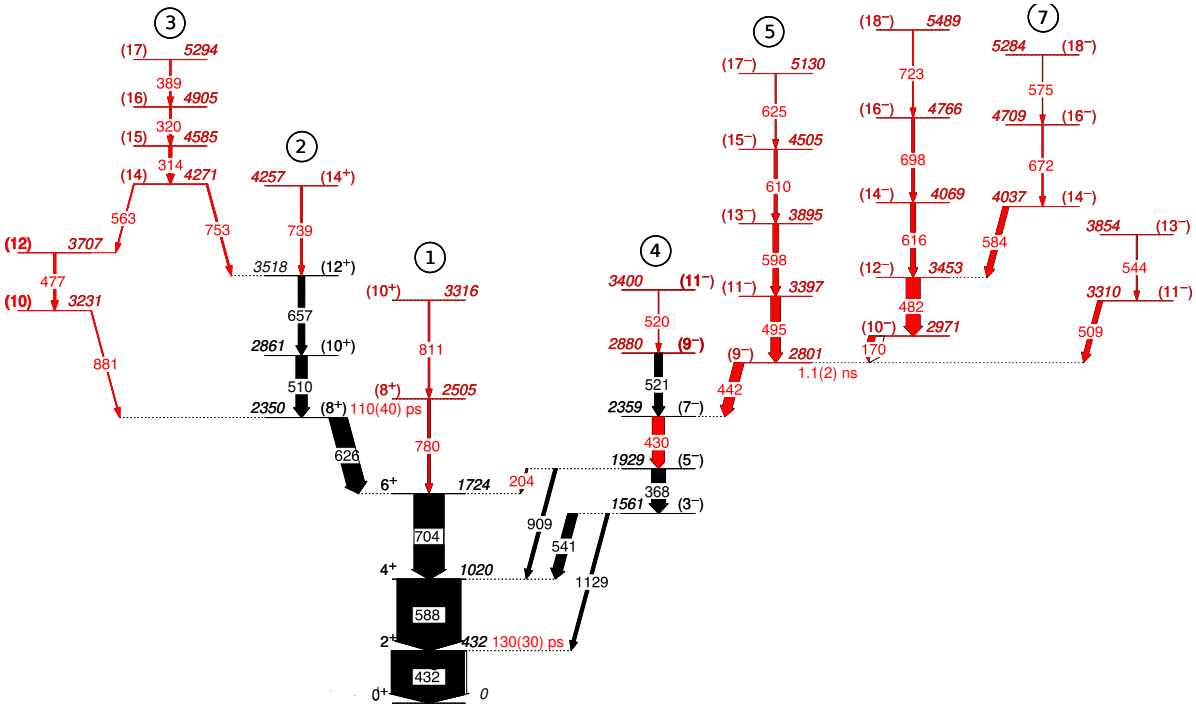

Figure 2. The level scheme for ^{166}Os. The transition energies are given in keV and the widths of the arrows correspond to the relative intensities of the transitions. The levels are labelled with their spin and parity and the excitation energy with respect to the ground state is given in keV. The parentheses indicate tentative spin and parity assignments. The new data are shown in red.

3.2. Mean Lifetime Measurements

The second experiment was dedicated to lifetime measurements of excited states with the Recoil Distance Doppler-Shift (RDDS) technique. The lifetimes of the yrast 2^+ and 8^+ states were extracted using the Differential Decay Curve Method (DDCM) [25]. The lifetimes of the 6^+ and 4^+ states could not be measured due to the feeding from the 2350 keV 8^+ state, which is slow compared with the lifetimes of the 6^+ and 4^+ states. In the DDCM, the lifetime is obtained from the intensity of the shifted (s) and degraded (d) components of the depopulating transition (dep) and the feeding transition (feed) according to

$$\tau(x) = \frac{1}{v} \frac{R^{\mathrm{d}}_{\mathrm{dep}}(x) - R^{\mathrm{d}}_{\mathrm{feed}}(x)}{\frac{\mathrm{d}}{\mathrm{d}x} R^{\mathrm{s}}_{\mathrm{dep}}(x)}, \tag{1}$$

where $R^{\mathrm{s}}_{\mathrm{dep}}(x) = {}^{I^{\mathrm{s}}_{\mathrm{dep}}(x)}/_{\left(I^{\mathrm{s}}_{\mathrm{dep}}(x)+I^{\mathrm{d}}_{\mathrm{dep}}(x)\right)}$ is the fraction of the shifted component of the depopulating transition from the level of interest and v is the velocity of the nucleus after the target. The mean lifetime τ is analyzed separately for each target-to-degrader distance x within the region of sensitivity, where both the numerator and the absolute value of the denominator in equation (1) are significantly larger than zero.

The lifetime of the 2^+ state was extracted using the α-decay correlated γ-ray

coincidences. Summed coincidences of the 510, 626 or 704 keV γ-ray transitions in the yrast band were demanded; both the depopulating transition of 432 keV and the feeding transition of 588 keV were fitted in these spectra. These coincidences were chosen to provide sufficient statistics for the peak fitting procedure and to reduce the influence of the 430 keV $(7^-) \rightarrow (5^-)$ γ-ray transition on the 2^+ lifetime measurement. It was not possible to demand coincidences so that all the feeding from the negative-parity band could be eliminated. Instead, coincidences with the 704 keV γ ray had to be included in order to obtain sufficient statistics for peak fitting and so feeding via the 204 keV γ-ray transition is possible. In addition, the feeding intensity originating from the $(7^-) \rightarrow (5^-)$ γ-ray transition, due to 510 and 626 keV being doublets with 509 and 625 keV, cannot be completely excluded. The 1129 keV γ-ray transition bypasses the 4^+ state and feeds the 2^+ state directly. Nevertheless, this weak branch feeding directly the 2^+ state does not significantly modify the time structure of the total feeding intensity since the lifetime of the 4^+ state is short compared with its feeding transitions, especially that from the 9^- state. The intensity of the 430 keV transition was determined to be less than 7% compared with that of the 432 keV transition from the intensity of the 204, 541 and 909 keV γ-ray peaks. The 442 keV γ-ray peak, which has half of the intensity of the 430 keV peak, is fitted in figure 3 to give an indication of the level of contamination. It is concluded that the overlapping 430 keV transition does not affect to the lifetime determination of the 2^+ state due to its weak intensity, which would limit the effect within the statistical uncertainty of the 2^+ state lifetime. The lifetimes were extracted from the measured γ-ray intensities using equation (1) separately for the three rings with $\theta = 71°$, $\theta = 109°$ and $\theta = 133°$. An example of the spectra for the 432 keV $2^+ \rightarrow 0^+$ transition recorded at $\theta = 71°$ is shown in the figure 3 with the resulting decay curve according to DDCM and the measured mean lifetimes.

The lifetime of the 2350 keV 8^+ state was analysed from the α-decay correlated singles γ-ray spectra. Only the feeding intensity via the 510 keV γ-ray transition was taken into account. The unobserved feeding was assumed to have a similar time behaviour to that of the observed one. For the 510 keV transition the fully shifted γ-ray intensity distribution is weighted to the shortest target-to-degrader distances. Although no lifetime for the 10^+ state can be extracted, one can conclude that the 510 keV transition is significantly faster than the 626 keV one. The feeding is extracted from the intensity of the degraded component (see equation (1)) and the sensitive target-to-degrader distances of the 510 keV and 626 keV transitions differ by an order of magnitude. Therefore, one can conclude that the 509 keV γ-ray does not have an effect on the lifetime of the 8^+ state.

The lifetime of the 2801 keV (9^-) state was too long to be determined precisely with the plunger device and only an estimate in the range $0.5 - 2$ ns was obtained. A more precise value was obtained using the recoil shadow anisotropy method (RSAM) [26]. In RSAM, the anisotropy A_γ extracted from the measured γ-ray intensities with the clover crystals around $\theta = 90°$ and determined as

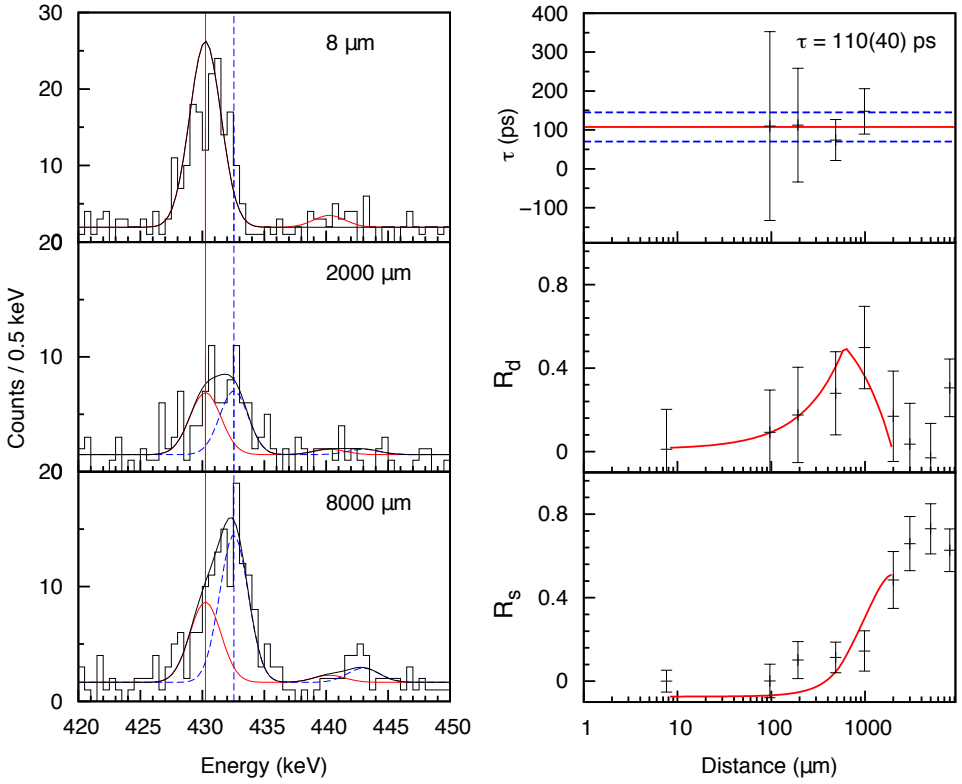

Figure 3. Left hand panel: Alpha-decay correlated γ-ray spectra in coincidence with the 510, 626 or 704 keV γ rays and the fits for the 432 keV $2^+ \rightarrow 0^+$ transition recorded at $\theta = 71^\circ$ are shown. The blue line marks the fit of the shifted component and the red line that of the degraded component. Also the 442 keV peak is fitted to indicate the intensity of the $(9^-) \rightarrow (7^-)$ transition. The spectra are Doppler corrected in energy with the velocity of the nuclei after the target. The right hand panel shows the mean lifetimes and the decay curves for the 432 keV $2^+ \rightarrow 0^+$ transition extracted using the DDCM.

$$A_\gamma = \frac{I(\theta = 71^\circ) - I(\theta = 80^\circ) + I(\theta = 100^\circ) - I(\theta = 109^\circ)}{I(\theta = 71^\circ) + I(\theta = 80^\circ) + I(\theta = 100^\circ) + I(\theta = 109^\circ)}, \tag{2}$$

is used to calculate the lifetime from

$$A_\gamma = \int_0^\infty A_{\rm det}(x)\epsilon(x)P(x)\mathrm{d}x, \tag{3}$$

where $A_{\rm det}$ is the detector asymmetry at a distance x after the target and $\epsilon(x)$ is the relative efficiency of the γ-ray detection at the distance x, $P(x)$ is the probability of the nucleus emitting a γ ray at the distance x after the target and it is related to the lifetime τ of the state and the velocity of the recoiling nucleus. Figure 4 compares the $\alpha(^{166}\mathrm{Os})$-decay correlated γ rays detected in the Clover detectors with the measured asymmetry spectrum. Only the experimental data with the shortest target-to-degrader distance of 8 µm was used to determine the asymmetry. Gamma rays emitted promptly at the target position should have zero asymmetry. The criterion was confirmed to be valid with a test using the 170 keV $(10^- \rightarrow 9^-)$ γ-ray transition, which yielded an asymmetry of $A_\gamma(170\,\mathrm{keV}) = 0.009(2)$. The detector efficiency was simulated with

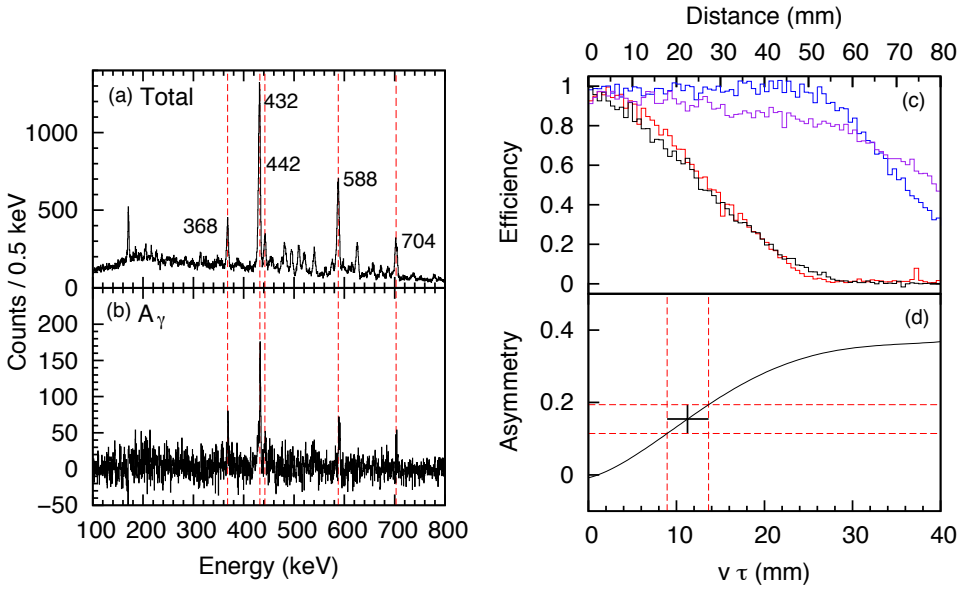

Figure 4. (a) Gamma rays detected in the JUROGAM II clover detectors in delayed coincidence with recoils implanted in the GREAT DSSD and followed by the characteristic α decay of ^{166}Os within the same pixel. The recoil-decay correlation time was restricted to 600 ms and measurements are restricted to the target-to-degrader distance of 5 µm. (b) The asymmetry spectrum defined by equation 2 for the 442 keV ($9^- \rightarrow 7^-$) transition. (c) The simulated relative efficiency as a function of distance behind the target for the clover detectors at $\theta = 71°$ (purple), $\theta = 80°$ (black), $\theta = 100°$ (blue), and $\theta = 109°$ (red) relative to the beam direction. (d) The calculated asymmetry as a function recoil velocity and the state lifetime. The extracted value for the (9^-) state is marked.

GEANT4 as a function of the distance from the target position, see figure 4(c). For the determination of the lifetime of the (9^-) state, the 442 keV γ-ray transition was used, as it depopulates the relatively long-lived (9^-) state. Figure 4(d) shows the integrated asymmetry according to equation 3 for different values of recoil velocity and lifetime ($v\tau$). The measured asymmetry of $A_\gamma(442\,\text{keV}) = 0.15(4)$ corresponds to a mean lifetime of 1100(200) ps.

The results of the lifetime measurements are presented in table 2.

Table 2. The mean lifetimes of the excited states and the reduced transition probabilities for the depopulating $E2$ transitions measured in the present work. The lifetimes of the 2^+, 8^+ states have been extracted with the RDDS method and the lifetime of the (9^-) state has been obtained with the RSAM analysis.

Level	τ (ps)	E_γ (keV)	$B(E2)(e^2\text{b}^2)$	$B(E2)$(W.u.)
2^+	130(30)	432.0	0.042(10)	7(2)
8^+	110(40)	626.1	0.008(3)	1.4(5)
(9^-)	1100(200)	442.4	0.0042(8)	0.77(15)

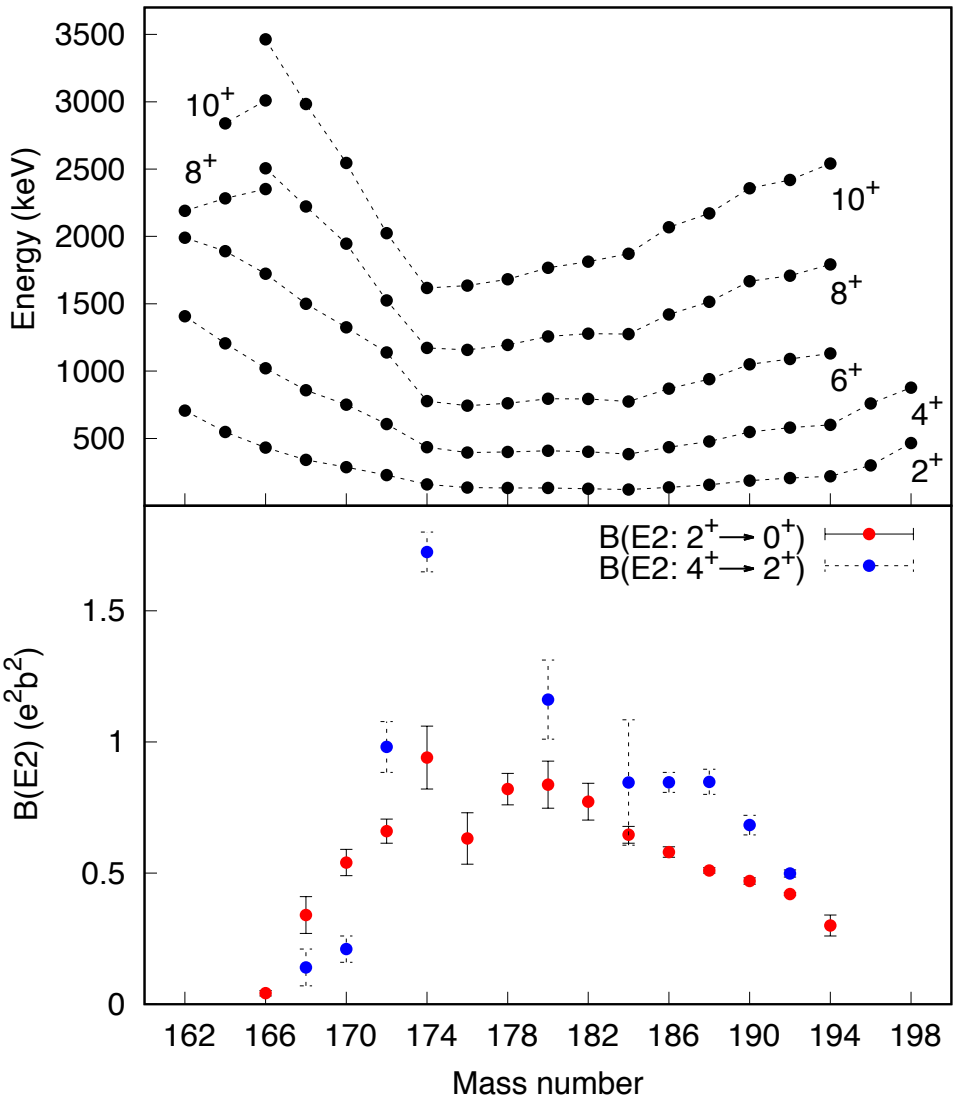

Figure 5. (a) Energies of the 2^+, 4^+, 6^+, 8^+ and 10^+ states in osmium isotopes. (b) The corresponding $B(E2; 2^+ \rightarrow 0^+)$ and $B(E2; 4^+ \rightarrow 2^+)$ values. Data taken from [1, 23, 27, 28, 29, 30, 31, 32, 33, 34, 35, 36, 37, 38, 39, 40, 2, 5].

4. Discussion

The excitation energies of the lowest-lying excited states and the $B(E2)$ values of the $2^+ \rightarrow 0^+$ and $4^+ \rightarrow 2^+$ transitions in the Os nuclei are shown in figure 5. The excitation energies reach their minimum values near the neutron mid shell ($N = 104$) while, conversely, the $B(E2)$ values reach their maximum values. These features reflect the correlation between the number of valence neutrons and deformed nuclear shapes. The Os nuclei remain moderately deformed until the level energies start to increase at ^{196}Os, which is interpreted as a transition from axially symmetric to γ-unstable/triaxial rotors when approaching the $N = 126$ closed shell [40, 2].

The neutron-deficient Os isotopes have a different structure. The level energies

increase towards $N = 82$ as the $B(E2; I \rightarrow I-2)$ values decrease as the number of valence nucleons is reduced outside the $N = 82$ closed shell. However, based on the moderately low excitation energy of the 2^+ state one would expect the $2^+ \rightarrow 0^+$ transition in ^{166}Os to be collective with comparable $B(E2; 2^+ \rightarrow 0^+)$ values to that in ^{168}Os ($B(E2; 2^+ \rightarrow 0^+)$=74(13) W.u.) [6]. The present data for ^{166}Os yield value of $B(E2; 2^+ \rightarrow 0^+) = 7(2)$ W.u, which approaches a typical value for a non-collective single-particle transition. Similarly, low reduced transition probabilities of the order of 20 W.u. have been observed for the $4^+ \rightarrow 2^+$ and $12^+ \rightarrow 10^+$ transitions in ^{168}Os [6], and the $6^+ \rightarrow 4^+$ and $12^+ \rightarrow 10^+$ transitions in ^{166}W [7].

These features are hard to reconcile with theoretical calculations, which often predict higher $B(E2; 2^+ \rightarrow 0^+)$ and $B(E2; 4^+ \rightarrow 2^+)$ values. However, it is noted that recent theoretical calculations employing the Skyrme Hartree-Fock-Bogoliubov calculations with the Sly4 and UNEDF02 parameters in the transformed harmonic oscillator basis appear to reproduce the low collectivity of the $2^+ \rightarrow 0^+$ transition observed in the present work [41]. These predictions are promising albeit with the caveat that the model predicts $B(E2)$ values based on quadrupole deformation parameters calculated using the collective rotational model.

The level scheme exhibits features that can be interpreted in terms of single-particle excitations. The two 8^+ states were observed at similar excitation energies. The excitation energy systematics in figure 5 suggest that the 8^+ states are associated with different structures that cross at ^{166}Os. The 2505 keV 8^+ state is interpreted to be the non-yrast continuation of the ground-state band. A similar interpretation is made for the 3316 keV 10^+ state. The yrast 2350 keV 8^+ state marks the beginning of a trend towards lower 8^+ excitation energies towards ^{162}Os, which is the lightest Os nucleus where the excited states have been observed. The level spacing of the 6^+ and 8^+ states starts to resemble that stemming from the seniority scheme [9]. Indeed, a possibility that the 8^+ states in lighter Os nuclei would be part of the $\nu(h_{9/2})^2$ or $\nu(f_{7/2}h_{9/2})$ multiplet is discussed in Refs. [1, 23]. The observed transition rate $B(E2; 8^+ \rightarrow 6^+) = 1.4(5)$ W.u. suggests this transition has a single-particle nature.

In marked contrast, the alignment properties deduced from the level scheme shown in figure 6(a) suggest collective features for ^{166}Os, which constitutes an apparent contradiction with the low collectivity implied by the lifetime measurements. Figure 6 compares the behaviour of the high-spin structure of ^{166}Os with ^{168}Os in terms of the angular momentum of the initial emitting state I_i, as a function of the γ-ray energy, E_γ. This formulation is chosen over the familiar alignment plots as a function of rotational frequency since it relies entirely on raw data and removes the need to specify the K quantum number and reference, which is ill-defined in γ-soft triaxial nuclei like the heavy $N \sim 90$ nuclei.

Figure 6 shows that the ground-state band in ^{166}Os is crossed by an excited configuration. The angular momentum gain is smaller than observed in ^{168}Os, which is attributed to the rotational alignment of an $i_{13/2}$ quasineutron pair [42]. The $i_{13/2}$ quasineutrons have higher excitation energies relative to the Fermi surface at the lower

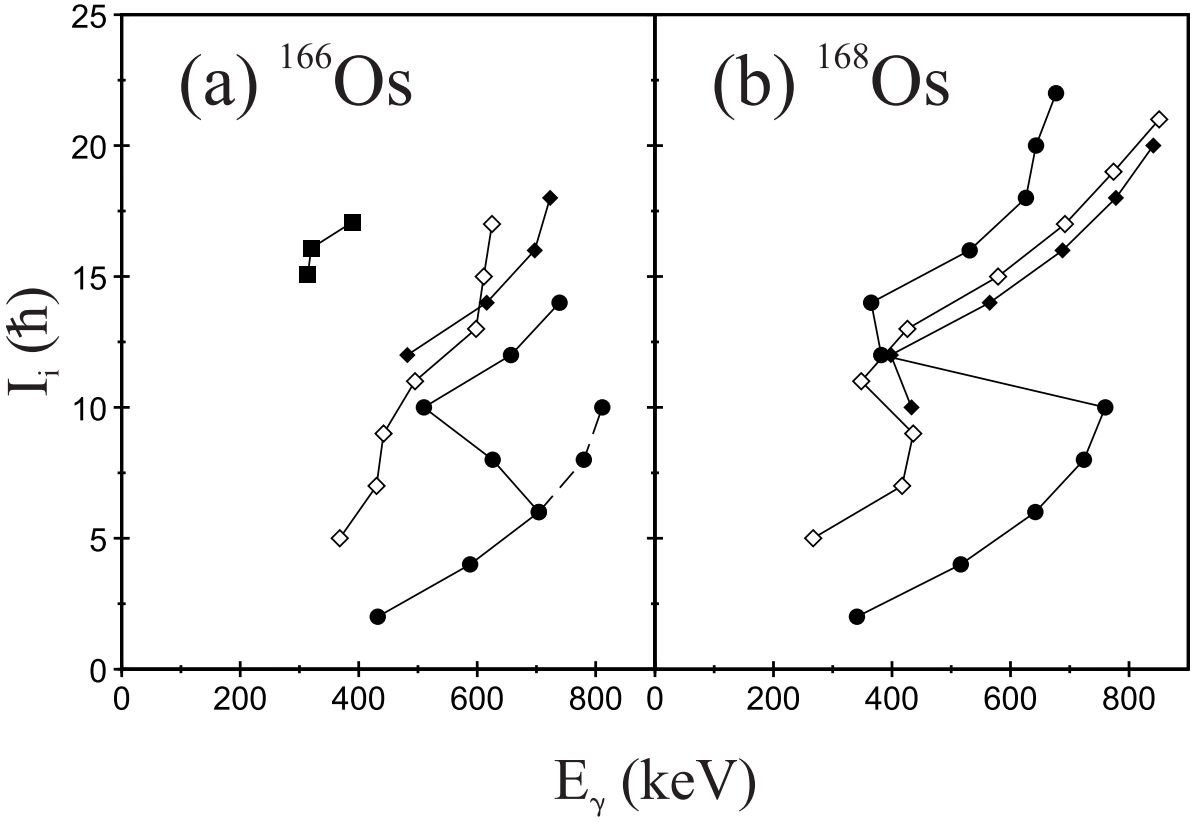

Figure 6. Angular momentum of the initial emitting state I_i versus γ-ray energy E_γ for bands in (a) ^{166}Os and (b) ^{168}Os. Filled circles correspond to the states with the (+,0) parity-signature configurations. Open diamonds represent bands 4 and 5 in ^{166}Os as a single sequence of parity-signature (−,+1), filled diamonds to band 6 (−,0) configuration, and the filled squares to the excited (+,0) configuration assigned to band 3 in ^{166}Os. The data for ^{168}Os is taken from Ref. [6].

deformation measured for ^{166}Os and alignments of the lowest negative-parity neutron pair are favoured. Hence band 2 is assigned to be based on the mixed $(h_{9/2})^2$ and $(h_{9/2}, f_{7/2})$ two-quasineutron configuration. Similar alignment properties are observed in other nuclei in the $N \sim 90$ mass region [43, 44, 45].

The lowest-lying negative-parity band in ^{166}Os (band 4) resembles those in nearby nuclei, which have been interpreted previously as structures arising from mixing with low-spin octupole vibrational bands [6, 27, 46, 44]. The low collectivity measured in ^{166}Os could also allow band 4 to be interpreted in terms of a $\nu(i_{13/2} \otimes f_{7/2})$ multiplet structure. This multiplet would produce the 3^-, 5^-, 7^- and 9^- states. The spin assignments of the low-lying negative-parity states remain tentative due to unreliable angular distributions due to dealigned states in the decay path from the (9^-) isomer at 2801 keV.

Bands 4 and 5 in ^{166}Os are treated as a single sequence of parity-signature (−,+1) in figure 6(a). At higher angular momentum band 5 (−,+1) and band 6 (−,0) have similar alignment properties to the low-lying negative-parity bands in ^{168}Os. These are

interpreted to be signature-partner bands formed by coupling a $i_{13/2}$ quasineutron with the lowest energy negative-parity $(h_{9/2}, f_{7/2})$ quasineutrons, respectively. Excited states at similar excitation energies could be formed by other configurations involving $i_{13/2}\otimes$ $(h_{9/2}, f_{7/2})$ pairs.

The alignment for the band at 4271 keV (band 3) is marginally higher than the $(i_{13/2})^2$ configuration that crosses the ground-state band in ^{168}Os. It is possible that this is a four-quasiparticle configuration formed by aligning the $h_{11/2}$ quasiprotons with the $\left(\nu h_{9/2}\right)^2$ quasineutrons although other couplings cannot be ruled out.

While it is well known that single-particle and collective excitations cannot be entirely decoupled from each other, the spectrum of excited states in the transitional nucleus ^{166}Os presents some intriguing features that can be interpreted in terms of both regimes. There have been interpretations of high-angular momentum data in heavy nuclei that suggest that the moments of inertia references used in rotational models vary systematically across isotopic chains and may allow reasonable collective descriptions for weakly deformed systems [47]. Further work from theoretical and experimental perspectives are needed to fully understand these unusual features.

5. Summary

The level scheme of ^{166}Os has been extended using recoil-decay tagged γ-ray spectroscopy to moderately high angular momentum ($I = 18$). The mean lifetimes of excited states have been measured with the RDDS and RSAM methods. The lifetime of the first 2^+ state was measured to be 130(30) ps and the corresponding reduced transition probability for the $2^+ \rightarrow 0^+$ transition is determined to be $B(E2; 2^+ \rightarrow 0^+) = 7(2)$ W.u. This value is markedly lower than the corresponding values for the heavier even-N Os isotopes and approaches the single-particle limit. The lifetimes for the 8^+ and 9^- states and the deduced reduced transition probabilities for their respective depopulating transitions also indicate single-particle transitions. These results and the anomalous ratios of reduced transition probabilities in the nearby even-even nuclei have been suggested to arise from the seniority scheme, which would be exceedingly unusual given the large number of valence nucleons in ^{166}Os. It is possible that triaxial shape and γ softness also have an effect on the unexpected $B(E2)$ values. Indeed, the yrast spectra have been shown to display characteristics that can be interpreted in terms of a simple collective framework. These apparently contradictory manifestations of single-particle and collective characteristics in the low-spin states of ^{166}Os appear to be a feature of the heavy transitional nuclei near $N \sim 90$ and merit further investigation.

Combining the new results with the recent work for ^{168}Os [6] and ^{166}W [7], seniority-like structures may be seen. This is unusual since these nuclei are not situated at the shell closures and certainly warrants further investigations. Furthermore, in the recent study of ^{172}Pt [4], a phase transition between single-particle and collective regimes has been proposed to generate $B(E2; 4^+ \rightarrow 2^+)/B(E2; 2^+ \rightarrow 0^+) < 1$.

Acknowledgments

This work has been supported through EURONS (European Commission contract no. RII3-CT-2004-506065), the Academy of Finland under the Finnish Centre of Excellence Programme 2006-2011 (Nuclear and Accelerator Based Physics contract 213503). The UK/France (STFC/IN2P3) Loan Pool and GAMMAPOOL network are acknowledged for the EUROGAM detectors of JUROGAM I and II. A. H. would like to thank the Slovak Research and Development Agency under contract No. APVV-20-0532, and Slovak grant agency VEGA (contract No. 2/0067/21).

References

[1] Joss D T, Lagergren K, Appelbe D E, Barton C J, Simpson J, Cederwall B, Hadinia B, Wyss R, Eeckhaudt S, Grahn T, Greenlees P T, Jones P M, Julin R, Juutinen S, Kettunen H, Leino M, Leppänen A P, Nieminen P, Pakarinen J, Rahkila P, Scholey C, Uusitalo J, Page R D, Paul E S and Wiseman D R 2004 *Phys. Rev. C* **70**(1) 017302 URL https://link.aps.org/doi/10.1103/PhysRevC.70.017302

[2] Podolyák Z, Steer S J, Pietri S, Xu F R, Liu H L, Regan P H, Rudolph D, Garnsworthy A B, Hoischen R, Górska M, Gerl J, Wollersheim H J, Kurtukian-Nieto T, Benzoni G, Shizuma T, Becker F, Bednarczyk P, Caceres L, Doornenbal P, Geissel H, Greębosz J, Kelic A, Kojouharov I, Kurz N, Montes F, Prokopowicz W, Saito T, Schaffner H, Tashenov S, Heinz A, Pfützner M, Jungclaus A, Balabanski D L, Brandau C, Bruce A M, Catford W N, Cullen I J, Dombrádi Z, Estevez E, Gelletly W, Ilie G, Jolie J, Jones G A, Kmiecik M, Kondev F G, Krücken R, Lalkovski S, Liu Z, Maj A, Myalski S, Schwertel S, Walker P M, Werner-Malento E and Wieland O 2009 *Phys. Rev. C* **79**(3) 031305 URL https://link.aps.org/doi/10.1103/PhysRevC.79.031305

[3] Paul E S, Woods P J, Davinson T, Page R D, Sellin P J, Beausang C W, Clark R M, Cunningham R A, Forbes S A, Fossan D B, Gizon A, Gizon J, Hauschild K, Hibbert I M, James A N, LaFosse D R, Lazarus I, Schnare H, Simpson J, Wadsworth R and Waring M P 1995 *Phys. Rev. C* **51** 78–87

[4] Cederwall B, Doncel M, Aktas O, Ertoprak A, Liotta R, Qi C, Grahn T, Cullen D M, Nara Singh B S, Hodge D, Giles M, Stolze S, Badran H, Braunroth T, Calverley T, Cox D M, Fang Y D, Greenlees P T, Hilton J, Ideguchi E, Julin R, Juutinen S, Raju M K, Li H, Liu H, Matta S, Modamio V, Pakarinen J, Papadakis P, Partanen J, Petrache C M, Rahkila P, Ruotsalainen P, Sandzelius M, Sarén J, Scholey C, Sorri J, Subramaniam P, Taylor M J, Uusitalo J and Valiente-Dobón J J 2018 *Phys. Rev. Lett.* **121**(2) 022502 URL https://link.aps.org/doi/10.1103/PhysRevLett.121.022502

[5] Goasduff A, Ljungvall J, Rodríguez T R, Bello Garrote F L, Etile A, Georgiev G, Giacoppo F, Grente L, Klintefjord M, Kuşoğlu A, Matea I, Roccia S, Salsac M D and Sotty C 2019 *Phys. Rev. C* **100**(3) 034302 URL https://link.aps.org/doi/10.1103/PhysRevC.100.034302

[6] Grahn T, Stolze S, Joss D T, Page R D, Sayğı B, O'Donnell D, Akmali M, Andgren K, Bianco L, Cullen D M, Dewald A, Greenlees P T, Heyde K, Iwasaki H, Jakobsson U, Jones P, Judson D S, Julin R, Juutinen S, Ketelhut S, Leino M, Lumley N, Mason P J R, Möller O, Nomura K, Nyman M, Petts A, Peura P, Pietralla N, Pissulla T, Rahkila P, Sapple P J, Sarén J, Scholey C, Simpson J, Sorri J, Stevenson P D, Uusitalo J, Watkins H V and Wood J L 2016 *Phys. Rev. C* **94**(4) 044327 URL https://link.aps.org/doi/10.1103/PhysRevC.94.044327

[7] Sayğı B, Joss D T, Page R D, Grahn T, Simpson J, O'Donnell D, Alharshan G, Auranen K, Bäck T, Boening S, Braunroth T, Carroll R J, Cederwall B, Cullen D M, Dewald A, Doncel M, Donosa L, Drummond M C, Ertuğral F, Ertürk S, Fransen C, Greenlees P T, Hackstein M, Hauschild K, Herzan A, Jakobsson U, Jones P M, Julin R, Juutinen S, Konki J, Kröll T, Labiche

M, Lopez-Martens A, McPeake C G, Moradi F, Möller O, Mustafa M, Nieminen P, Pakarinen J, Partanen J, Peura P, Procter M, Rahkila P, Rother W, Ruotsalainen P, Sandzelius M, Sarén J, Scholey C, Sorri J, Stolze S, Taylor M J, Thornthwaite A and Uusitalo J 2017 *Phys. Rev. C* **96**(2) 021301 URL https://link.aps.org/doi/10.1103/PhysRevC.96.021301

[8] Lewis M, Joss D, Sayğı B, Page R, Cullen D, Barber L, Giles M, Simpson J, Al-Aqeel M, Badran H, Braunroth T, Briscoe A, Calverley T, Dewald A, Doncel M, Grahn T, Greenlees P, Henrich C, Herzáň A, Herzberg R D, Higgins E, Hilton J, Ilieva S, Julin R, Juutinen S, Keatings J, Kröll T, Labiche M, Mashtakov K, Singh B N, Parr E, Partanen J, Paul E, Rahkila P, Sandzelius M, Sarén J, Scholey C, Siciliano M, Spagnoletti P, Stolze S, Szwec S, Taylor M and Uusitalo J 2019 *Physics Letters B* **798** 134998 ISSN 0370-2693 URL http://www.sciencedirect.com/science/article/pii/S0370269319307208

[9] DeShalit A 1963 *Nuclear shell theory* Pure and applied physics (New York,)

[10] Talmi I 1971 *Nucl. Phys. A* **172** 1

[11] Beausang C W, Forbes S A, Fallon P, Nolan P J, Twin P J, Mo J N, Lisle J C, Bentley M A, Simpson J, Beck F A, Curien D, deFrance G, Duchêne G and Popescu D 1992 *Nuclear Instruments and Methods in Physics Research Section A: Accelerators, Spectrometers, Detectors and Associated Equipment* **313** 37 – 49

[12] Alvarez C R 1993 *Nucl. Phys. News* **3**

[13] Leino M, Äystö J, Enqvist T, Heikkinen P, Jokinen A, Nurmia M, Ostrowski A, Trzaska W H, Uusitalo J, Eskola K, Armbruster P and Ninov V 1995 *Nuclear Instruments and Methods in Physics Research Section B: Beam Interactions with Materials and Atoms* **99** 653 – 656

[14] Sarén J, Uusitalo J, Leino M and Sorri J 2011 *Nuclear Instruments and Methods in Physics Research Section A: Accelerators, Spectrometers, Detectors and Associated Equipment* **654** 508 – 521 ISSN 0168-9002 URL http://www.sciencedirect.com/science/article/pii/S0168900211011922

[15] Page R D, Andreyev A N, Appelbe D E, Butler P A, Freeman S J, Greenlees P T, Herzberg R D, Jenkins D G, Jones G D, Jones P, Joss D T, Julin R, Kettunen H, Leino M, Rahkila P, Regan P H, Simpson J, Uusitalo J, Vincent S M and Wadsworth R 2003 *Nuclear Instruments and Methods in Physics Research Section B: Beam Interactions with Materials and Atoms* **204** 634 – 637

[16] Lazarus I H, Appelbe D E, Butler P A, Coleman-Smith P J, Cresswell J R, Freeman S J, Herzberg R D, Hibbert I M, Joss D T, Letts S C, Page R D, Pucknell V F E, Regan P H, Sampson J, Simpson J, Thornhill J and Wadsworth R 2001 *Nuclear Science, IEEE Transactions on* **48** 567 –569

[17] Rahkila P 2008 *Nuclear Instruments and Methods in Physics Research Section A: Accelerators, Spectrometers, Detectors and Associated Equipment* **595** 637 – 642

[18] Radford D C 1995 *Nuclear Instruments and Methods in Physics Research Section A: Accelerators, Spectrometers, Detectors and Associated Equipment* **361** 306 – 316 ISSN 0168-9002 URL http://www.sciencedirect.com/science/article/pii/0168900295001840

[19] Radford D C 1995 *Nuclear Instruments and Methods in Physics Research Section A: Accelerators, Spectrometers, Detectors and Associated Equipment* **361** 297 – 305 ISSN 0168-9002 URL http://www.sciencedirect.com/science/article/pii/0168900295001832

[20] Duchêne G, Beck F A, Twin P J, de France G, Curien D, Han L, Beausang C W, Bentley M A, Nolan P J and Simpson J 1999 *Nuclear Instruments and Methods in Physics Research Section A: Accelerators, Spectrometers, Detectors and Associated Equipment* **432** 90 – 110

[21] Taylor M J, Cullen D M, Smith A J, McFarlane A, Twist V, Alharshan G A, Procter M G, Braunroth T, Dewald A, Ellinger E, Fransen C, Butler P A, Scheck M, Joss D T, Sayği B, McPeake C G, Grahn T, Greenlees P T, Jakobsson U, Jones P, Julin R, Juutinen S, Ketelhut S, Leino M, Nieminen P, Pakarinen J, Peura P, Rahkila P, Ruotsalainen P, Sandzelius M, Sarén J, Scholey C, Sorri J, Stolze S and Uusitalo J 2013 *Nuclear Instruments and Methods in Physics Research Section A: Accelerators,*

Spectrometers, Detectors and Associated Equipment **707** 143 – 148 ISSN 0168-9002 URL http://www.sciencedirect.com/science/article/pii/S0168900213000028

[22] Baglin C M 2008 *Nuclear Data Sheets* **109** 1103 ISSN 0090-3752 URL http://www.sciencedirect.com/science/article/pii/S009037520800029X

[23] King S L, Page R D, Simpson J, Keenan A, Amzal N, Chewter A J, Cocks J F C, Cullen D M, Dorvaux O, Greenlees P T, Helariutta K, Jones P, Joss D T, Julin R, Juutinen S, Kankaanpää H, Kettunen H, Kuusiniemi P, Leino M, Lemmon R C, Muikku M, Nieminen P, Savelius A, Shepherd S L, Smith M B, Taylor M J and Uusitalo J 2000 *Phys. Rev. C* **62**(6) 067301 URL http://link.aps.org/doi/10.1103/PhysRevC.62.067301

[24] Appelbe D E, Simpson J, Muikku M, Boardman H J, Melarangi A, Page R D, Greenlees P T, Jones P M, Julin R, Juutinen S, Keenan A, Kettunen H, Kuusiniemi P, Leino M, Nieminen P, Pakarinen J, Rahkila P, Uusitalo J and Joss D T 2002 *Phys. Rev. C* **66**(1) 014309 URL http://link.aps.org/doi/10.1103/PhysRevC.66.014309

[25] Dewald A, Harissopulos S and von Brentano P 1989 *Zeitschrift für Physik A Hadrons and Nuclei* **334**(2) 163–175

[26] Gueorguieva E, Kaci M, Schück C, Minkova A, Vieu C, Correia J J and Dionisio J S 2001 *Nuclear Instruments and Methods in Physics Research Section A: Accelerators, Spectrometers, Detectors and Associated Equipment* **474** 132 – 142 ISSN 0168-9002 URL http://www.sciencedirect.com/science/article/pii/S0168900201008774

[27] Dracoulis G D, Bark R A, Stuchbery A E, Byrne A P, Baxter A M and Riess F 1988 *Nuclear Physics A* **486** 414 – 428 ISSN 0375-9474 URL http://www.sciencedirect.com/science/article/pii/0375947488902448

[28] Davidson P M, Dracoulis G D, Kibedi T, Byrne A P, Anderssen S S, Baxter A M, Fabricius B, Lane G J and Stuchbery A E 1994 *Nuclear Physics A* **568** 90 – 106 ISSN 0375-9474

[29] Browne E and Junde H 1999 *Nucl. Data Sheets* **87** 15

[30] Basunia M 2006 *Nucl. Data Sheets* **107** 791

[31] Achterberg E, Capurro O and Marti G 2009 *Nucl. Data Sheets* **110** 1473

[32] McCutchan E A 2015 *Nucl. Data Sheets* **126** 151

[33] Singh B 2015 *Nucl. Data Sheets* **130** 21

[34] Baglin C M 2010 *Nucl. Data Sheets* **111** 275

[35] Baglin C M 2003 *Nucl. Data Sheets* **99** 1

[36] Singh B 2002 *Nucl. Data Sheets* **95** 387

[37] Singh B 2003 *Nucl. Data Sheets* **99** 275

[38] Baglin C M 2012 *Nucl. Data Sheets* **113** 1871

[39] Daniel T, Kisyov S, Regan P H, Marginean N, Podolyák Z, Marginean R, Nomura K, Rudigier M, Mihai R, Werner V, Carroll R J, Gurgi L A, Oprea A, Berry T, Serban A, Nita C R, Sotty C, Suvaila R, Turturica A, Costache C, Stan L, Olacel A, Boromiza M and Toma S 2017 *Phys. Rev. C* **95**(2) 024328 URL https://link.aps.org/doi/10.1103/PhysRevC.95.024328

[40] John P R, Modamio V, Valiente-Dobón J J, Mengoni D, Lunardi S, Rodríguez T R, Bazzacco D, Gadea A, Wheldon C, Alexander T, de Angelis G, Ashwood N, Barr M, Benzoni G, Birkenbach B, Bizzeti P G, Bizzeti-Sona A M, Bottoni S, Bowry M, Bracco A, Browne F, Bunce M, Camera F, Cederwall B, Corradi L, Crespi F C L, Désesquelles P, Eberth J, Farnea E, Fioretto E, Görgen A, Gottardo A, Grebosz J, Grente L, Hess H, Jungclaus A, Kokalova T, Korichi A, Korten W, Kuşoğlu A, Lenzi S, Leoni S, Ljungvall J, Maron G, Meczynski W, Melon B, Menegazzo R, Michelagnoli C, Mijatović T, Million B, Molini P, Montagnoli G, Montanari D, Napoli D R, Nolan P, Oziol C, Podolyák Z, Pollarolo G, Pullia A, Quintana B, Recchia F, Reiter P, Roberts O J, Rosso D, Şahin E, Salsac M D, Scarlassara F, Sferrazza M, Simpson J, Söderström P A, Stefanini A M, Stezowski O, Szilner S, Theisen C, Ur C A and Walshe J 2014 *Phys. Rev. C* **90**(2) 021301 URL https://link.aps.org/doi/10.1103/PhysRevC.90.021301

[41] Doncel M, Cederwall B, Qi C, Li H, Jakobsson U, Auranen K, Bönig S, Drummond M C, Grahn T, Greenlees P T, Herzan A, Joss D T, Julin R, Juutinen S, Konki J, Kröll T, Leino M, McPeake C,

O'Donnell D, Page R D, Pakarinen J, Partanen J, Peura P, Rahkila P, Ruotsalainen P, Sandzelius M, Sarén J, Sayğı B, Scholey C, Sorri J, Stolze S, Taylor M J, Thornthwaite A and Uusitalo J 2017 *Phys. Rev. C* **95**(4) 044321 URL https://link.aps.org/doi/10.1103/PhysRevC.95.044321

[42] Joss D T, King S L, Page R D, Simpson J, Keenan A, Amzal N, Bäck T, Bentley M A, Cederwall B, Cocks J F C, Cullen D M, Greenlees P T, Helariutta K, Jones P M, Julin R, Juutinen S, Kankaanpää H, Kettunen H, Kuusiniemi P, Leino M, Muikku M, Savelius A, Uusitalo J and Williams S J 2001 *Nuclear Physics A* **689** 631 – 654 ISSN 0375-9474 URL http://www.sciencedirect.com/science/article/pii/S0375947400006928

[43] Lagergren K, Joss D T, , Paul E S, , Cederwall B, Simpson J, Appelbe D E, Barton C J, Eeckhaudt S, Grahn T, Greenlees P T, Hadinia B, Jones P, Julin R, Juutinen S, Kettunen H, Leino M, Leppänen A P, Nieminen P, Page R D, Pakarinen J, Perkowski J, Rahkila P, Scholey C, Uusitalo J, Wiseman D R, Warner D D and Wyss R 2011 *Phys. Rev. C* **83** 014313

[44] Joss D T, Dracoulis G D, Higgins E, Lewis M, Thomson J, Lane G J, Page R D, Simpson J, Bianco L, Cederwall B, Darby I G, Davidson P M, Eeckhaudt S, Ertürk S, Fabricius B, Gómez-Hornillos M B, Grahn T, Greenlees P T, Hadinia B, Jakobsson U, Jones P M, Julin R, Juutinen S, Ketelhut S, Leino M, Nieminen P, Nyman M, Pakarinen J, Paul E S, Peura P, Rahkila P, Ruotsalainen P, Sandzelius M, Sapple P J, Sarén J, Scholey C, Sorri J and Uusitalo J 2016 *Phys. Rev. C* **93**(2) 024307 URL https://link.aps.org/doi/10.1103/PhysRevC.93.024307

[45] Joss D T 2016 *EPJ Web of Conferences* **123** 01006

[46] Joss D T, Simpson J, Appelbe D E, Lagergren K, Barton C J, Cederwall B, Eeckhaudt S, Grahn T, Jones P M, Julin R, Juutinen S, Hadinia B, Kettunen H, Leino M, Leppänen A P, Nieminen P, Page R D, Pakarinen J, Paul E S, Perkowski J, Rahkila P, Riley M A, Scholey C, Uusitalo J, de Vel K V, Warner D D and Wiseman D R 2005 *Journal of Physics G: Nuclear and Particle Physics* **31** S1715 URL http://stacks.iop.org/0954-3899/31/i=10/a=060

[47] Rowley N, Ollier J and Simpson J 2009 *Phys. Rev. C* **80** 024323